



## Experimental Procedure

### Electrodes

Low hydrogen iron powder E10018-M and E12018-M electrodes from standard production were used. The core wire diameter was, in both cases, 4 mm and the coating factors D/d (coating diameter/wire diameter) were 1.65 and 1.70, respectively. The electrodes were redried for one hour at 350°C (662°F) before being used to uniform the starting conditions. (This was done because the electrodes belonged to standard batches of two different consumables, elaborated in different occasions, originally dried in production at 420°C (788°F) and packed in polyethylene bags and cardboard boxes.)

### Weld Preparation

The weld preparation for all test specimens was per AWS A5.5-81, using base metal thickness of  $\frac{1}{4}$  in. (19 mm). Welding was performed in the flat position and two beads per layer were deposited with only one for the first layer, as per the standard.

**Table 1 — AWS A5.5-81 E10018-M and E12018-M Electrode Tensile Property Requirements\***

Electrode	Tensile Strength (MPa)	Yield Strength (MPa)	Elongation (%)	Charpy V-Notch Impact at -51°C (J)
E10018-M	690	610-690	20	27
E12018-M	830 min	745-830	18 min	27 min

\*ANSI/AWS A5.5-96 requires the same all-weld metal mechanical property values.

The welding parameters employed for the six test assemblies (one set of three test assemblies with E10018-M and another set of three with E12018-M electrodes) are presented in Table 2, as well as the heat inputs that were used. The preheat and interpass temperatures were chosen always to be within the range established by the AWS A5.5-81 standard. Welding speed was determined by measuring bead length vs. arc time. The variation found in speed determination along the test coupon welding was maximum  $\pm 12\%$ .

### Mechanical Testing

From each test assembly, one tensile specimen (with a 4:1 gage length to diameter ratio and located exactly as required by AWS A5.5-81), one section for metallographic studies and five Charpy V-notch specimens were obtained. Tensile and toughness properties were tested in the as-welded condition, at room temperature and at -51°C (-60°F), respectively. Hardness Vickers (HV10) was measured from the top and along the center line of the metallographic specimen.

**Table 2 — Welding Parameters**

Electrode	E10018-M			E12018-M			AWS
	Hot	Medium	Cold	Hot	Medium	Cold	
Condition							—
Heat input (KJ/mm)	2.1	1.7	1.3	2.1	1.6	1.2	—
Amperage (A)	185	160	140	180	160	130	—
Arc voltage (V)	25	24	22	23	23	22	—
Interpass temperature (°C)	107	101	93	107	101	93	93-107
Welding speed (mm/s)	2.2	2.3	2.4	2.0	2.3	2.4	—
Number of layers	7	8	8	7	8	9	7-9

**Table 3 — All-Weld-Metal Chemical Composition Results and AWS Requirements**

Electrode	Heat Input (KJ/mm)										O (ppm)	N (ppm)
		C	Mn	P	S	Si	Ni	Cr	Mo	V		
E10018-M	Hot	0.042	1.34	0.025	0.013	0.34	1.90	0.08	0.38	<0.010	552	129
	Medium	0.041	1.45	0.028	0.013	0.40	1.97	0.08	0.40	<0.010	538	120
	Cold	0.056	1.49	0.029	0.013	0.40	1.97	0.09	0.40	<0.010	511	87
AWS requirements*		0.10	0.75-1.70	0.030	0.030	0.60	1.40-2.10	0.35	0.25-0.50	0.05		
E11018M (Ref. 1)	Hot	0.040	1.58	0.015	0.007	0.44	1.94	0.30	0.34	<0.010	361	84
		0.040	1.57	0.015	0.007	0.44	1.94	0.30	0.32	<0.010	360	88
	Medium	0.051	1.60	0.014	0.008	0.48	1.86	0.29	0.32	<0.010	321	84
		0.043	1.63	0.016	0.007	0.48	1.97	1.31	0.35	<0.010		
	Cold	0.040	1.67	0.016	0.007	0.54	1.92	0.30	0.34	<0.010	321	76
0.050		1.70	0.016	0.009	0.54	2.04	0.32	0.34	<0.010	309	67	
AWS requirements*		0.010	1.30-1.80	0.030	0.030	0.60	1.25-2.50	0.40	0.25-0.50	0.05		
E12018-M	Hot	0.043	1.56	0.022	0.016	0.43	2.25	0.45	0.43	<0.010	377	98
	Medium	0.048	1.62	0.018	0.013	0.45	2.20	0.43	0.42	<0.010	349	95
	Cold	0.051	1.68	0.020	0.012	0.46	2.13	0.46	0.40	<0.010	314	87
AWS requirements*		0.10	1.30-2.25	0.030	0.030	0.60	1.75-2.50	0.30-1.40	0.30-0.55	0.05		

\*AWS A5.5-81 and ANSI/AWS A5.5-96 standards require the same values. Single values are maximum.

## Metallography

Examinations of transverse sections (etched in a 2% solution of nital) were carried out on the top beads and the adjacent supercritically reheated zones, as described previously (Refs. 2-4) and according to Ref. 7.

## Results

The tables and/or figures include results from E11018-M type electrode testing (Ref. 1), for discussion purposes.

**Table 4 — Percentages of Columnar and Refined Region All-Weld-Metal Lying Ahead of the Charpy V-Notch**

Electrode	Heat input (KJ/mm)	Columnar Zone (%)	Refined Zone (%)
E10018-M	2.1	25	75
	1.7	42	58
	1.3	55	45
E11018-M (Ref. 1)	2.2	18	85
	2.0	25	75
	1.6	42	58
E12018-M	2.1	36	64
	1.6	45	55
	1.2	50	50

**Table 5 — Prior Austenite Grain Size (Width) in the As-Deposited Columnar Regions of the Final Pass**

Electrode	Heat input (KJ/mm)	Width of Prior Austenite Grain ( $\mu$ )
E10018-M	2.1	140
	1.7	125
	1.3	110
E11018-M (Ref. 1)	2.2	216
	2.0	189
	1.6	159

Note: For E12018-M electrode, it was not possible to perform the measurement due to the loss of the grain boundary ferrite veins.

**Table 6 — Quantitative Survey of Different Microstructural Constituents within the Columnar Region of the Top Passes**

Electrode	Heat input (KJ/mm)	Acicular Ferrite (%)	Ferrite with Second Phase (%)	Primary Ferrite (%)
E10018-M	2.1	62	20	18
	1.7	58	16	26
	1.3	56	14	30
E11018-M (Ref. 1)	2.2	74	20	6
	2.0	72	19	9
	1.6	66	17	17
E12018-M	2.1	64	26	10
	1.6	62	25	13
	1.2	59	22	19

## Chemical Composition

The chemical analyses of the two sets of three all-weld-metal deposits are presented in Table 3.

All the compositions satisfied the requirements of AWS A5.5-81 (Ref. 5) Table 3 and were within the optimum ranges for each element and for each electrode type E10018-M and 12018-M, as was found in previous studies (Refs. 2-4).

The oxygen and nitrogen values increased with the heat input. The higher amperage and voltage might result in more O and N in the arc environment

(Refs. 8, 9) as more time was available for the weld pool to absorb O and N from the environment (Ref. 9).

It is interesting to note that, due to the different coating factor, mineral base and Mn content of the coating of the E10018-M and E12018-M commercial electrodes, two different levels of oxygen were achieved: 511 to 552 ppm and 314 to 377 ppm, respectively. In spite of that fact, both are iron powder basic coating electrodes according to EXXX18-X classification.

In both cases, it can be seen that as the heat input increased, the values of Mn and Si slightly decreased, due to the higher oxidation of these two elements, which are not only alloying elements but also deoxidants in the arc. This effect was previously found by Evans (Refs. 10, 11) and Vercesi, *et al.* (Ref. 1). The two test specimens, welded with the intermediate conditions, presented intermediate Mn and Si values.

As a general tendency, carbon figures decreased with the increase of the heat input for the same reasons.

## Metallographic Examination

### General

Table 4 presents the zonal distribution along the vertical central line, in the Charpy V-notch location with the three heat inputs employed, in the two sets. It can be seen that as the heat input decreased, the percentages of columnar zone increased, at the expense of the refined zones, as was shown before (Refs. 1, 10, 11).

### As-Deposited Weld Metal

Examination of as-deposited weld metal with low magnification revealed the width of the prior/columnar austenite grains increased as the heat input increased, Table 5, as previously indicated (Refs. 1, 10-12). The prior austenite grain size (width) in the as-deposited columnar regions of the final pass, was measured only for the E10018-M all-weld-metal. It was not possible to carry out the same measurement in E12018-M all-weld metal because the veins of grain boundary ferrite disappeared as the degree of alloy increased (addition of Cr and increment of Mn and Ni, Table 3), as shown earlier (Refs. 13-16).

The last deposited beads were examined at 100X and 200X and quantitative metallographic measurements were performed at 400X, identifying the following major microstructural components:

- primary ferrite
- acicular ferrite
- ferrite with second phase

With higher magnification, other constituents can be identified and quantified (Ref. 16).

In Table 6, the point count results are given; it can be observed that as the heat input increased, there was a slight increase of both acicular ferrite and ferrite with second phase, either aligned or non-aligned at the expense of primary ferrite. This is in accordance with previous results (Ref. 1).

Typical microphotographs of both electrodes columnar regions are shown in Fig. 1 for E10018-M (100X) and Fig. 2 for E12018-M (200X).

#### Reheated Weld Metal

It was not possible to differentiate the coarse from the fine refined zones or to measure the ferrite grain size because under the magnification used, it was too small; see the photomicrographs presented in Fig. 3A for E10018-M and Fig. 3B for E12018-M, both at 200X. However, the general decrease in ferrite grain size when the heat input decreased is noticeable.

#### Mechanical Properties

##### Hardness Testing

Average hardness values obtained from the metallographic sections, are presented in Fig. 4 for E10018-M and E12018-M electrodes.

With both electrodes, as the heat input increased, hardness values decreased, in accordance with previous studies (Refs. 1, 12, 17, 18). The figures obtained with the E12018-M electrodes are higher than those obtained with the E10018-M ones, as expected, due to the higher alloy content — Table 3. The values obtained before (Ref. 1) with E11018-M electrode are between those of E12018-M and E10018-M. It was not possible to explain the decline in hardness that appeared in the center of the transversal sections, for both electrodes, taking into account the variation of welding speed and other welding conditions, during the specimen welding.

##### Soundness Test Results

The two sets of three test assemblies were radiographed in accordance with AWS A5.5-81 (and also with ANSI/AWS A5.5-96) and presented optimum results — no apparent defects.

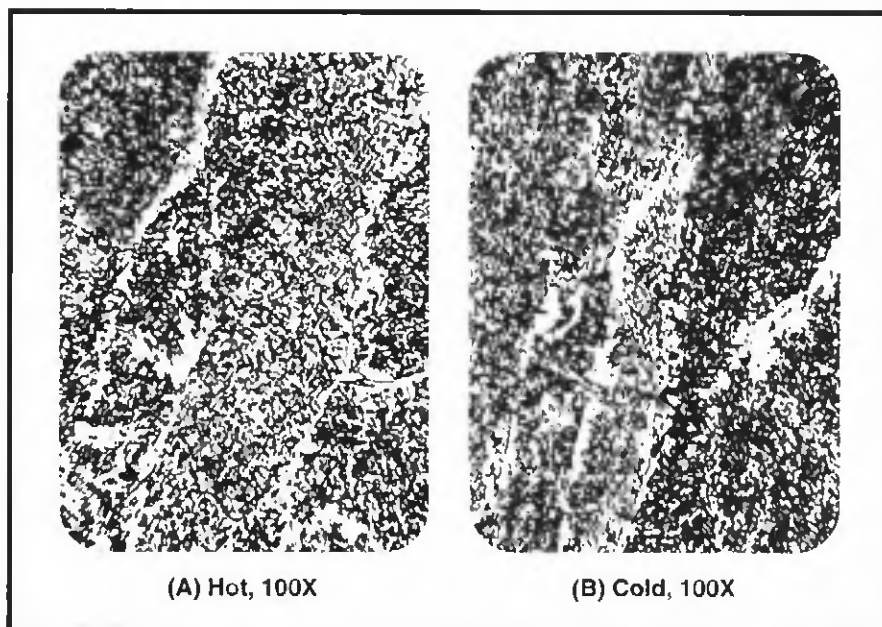


Fig. 1 — Photomicrographs of columnar zones (E10018-M): A — Hot 100X; B — Cold 100X.

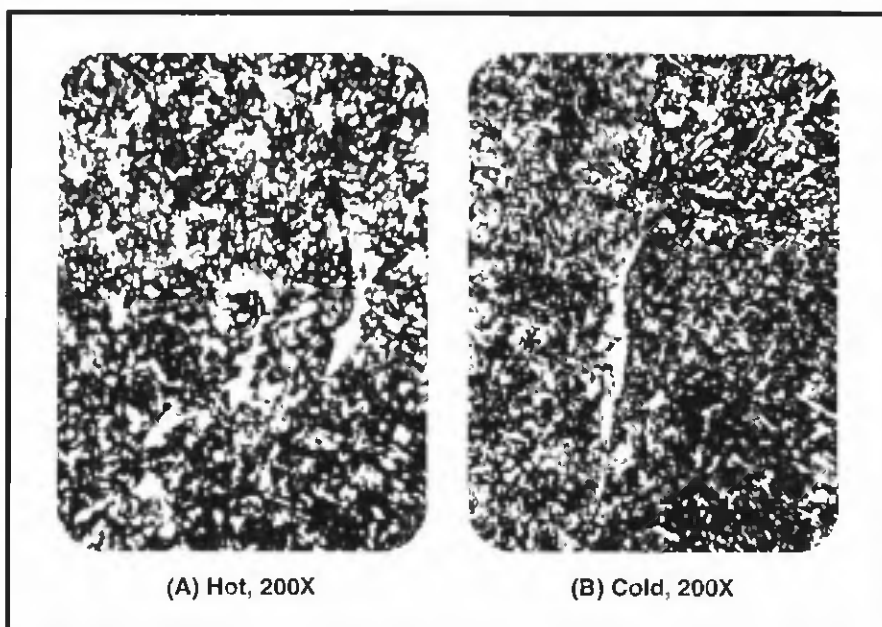


Fig. 2 — Photomicrographs of columnar zones (E12018-M): A — Hot 200X; B — Cold 200X.

##### Tensile Results

The tensile test data obtained for the six test assemblies, as well as the AWS requirements for each electrode, are presented in Table 7.

It generally can be observed that as the heat input increased, the tensile and yield strengths decreased, as previously found for E11018-M electrode (Ref. 1) and for similar high strength weld-metal obtained with different welding processes (Refs. 12, 17–20). With both electrodes and all the heat inputs, min-

imal elongation requirements were satisfied.

1) *E10018-M electrode*: with the three heat inputs, the obtained values of tensile properties were within the requirements of the AWS standard. Although the tensile properties varied according to the heat input that was used, this variation remained within the requirements of the AWS standard.

2) *E12018-M electrode*: only the medium specimen satisfied the AWS requirements. The cold specimen presented

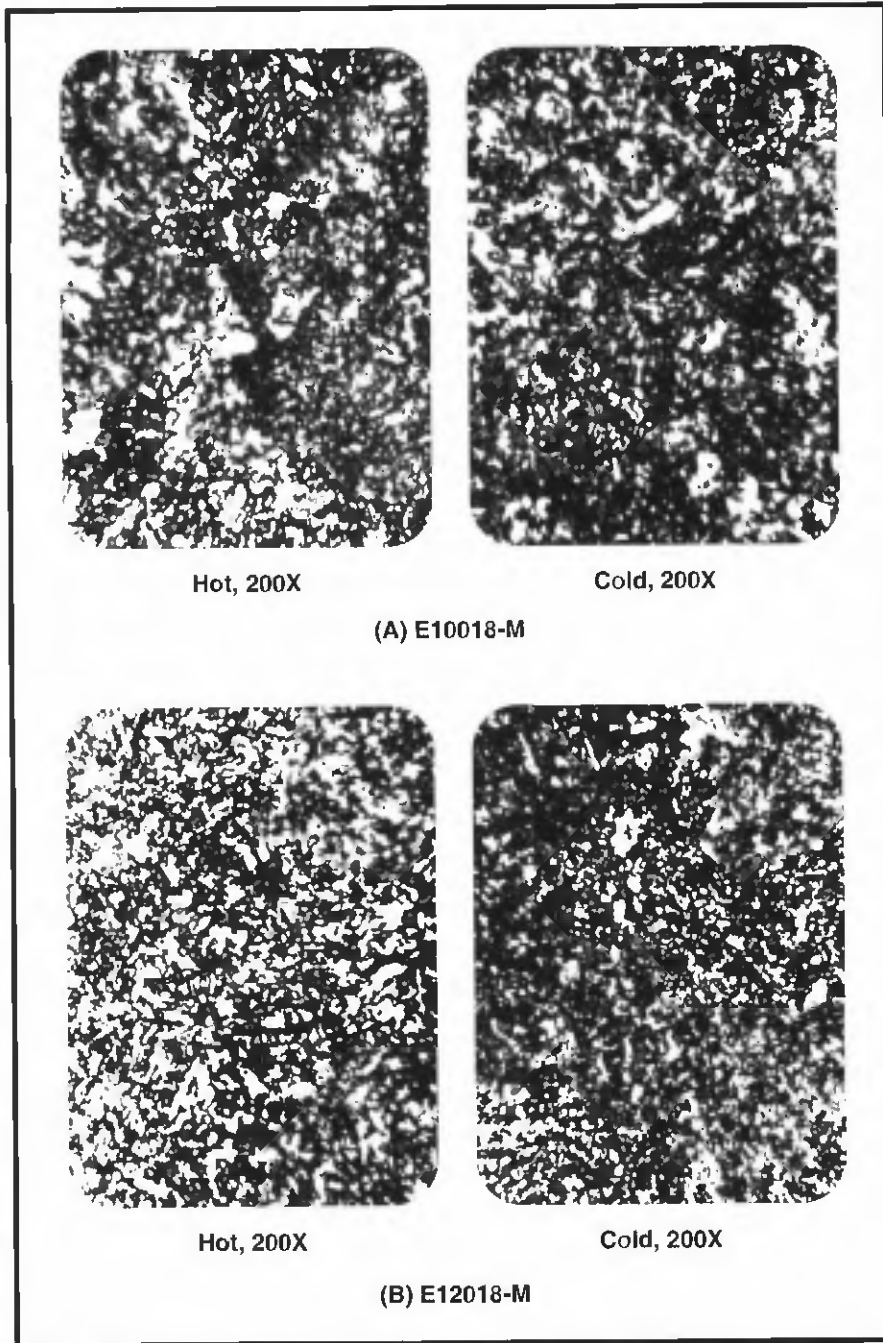


Fig. 3 — Photomicrographs of recrystallized zones: A — E10018-M, 200X; B — E12018-M, 200X.

yield strength that exceeded the maximum allowed and the hot one did not fulfill the minimal tensile strength required.

#### Impact Results

The Charpy-V impact values from the six test specimens are presented in Table 7. Values comfortably in excess of the minimum requirements were achieved with all the assemblies and there was not one value below the AWS minimal requirement. The average values were similar to those obtained with commercial

E10018/ E11018/ E12018-M type electrodes (Refs. 21, 22).

The difference in the all-weld metal oxygen contents obtained with E10018-M and E12018-M electrodes could have been reflected in a toughness increase for the second electrode, as it is recognized that oxygen content affects the distribution (Ref. 23) and quantity (Refs. 24, 25) of inclusions: lower oxygen concentrations result in smaller inclusion diameter and lower volume fraction. These last two facts, in turn, result in better toughness (Ref. 26). In the present case, the benefi-

cial lower oxygen content of E12018-M deposits may have been counteracted by the increase in tensile properties known to be deleterious to toughness (Ref. 27).

#### Discussion

It is well known that mechanical properties of low-alloy high-strength steel welds depend on their microstructure as well as on their chemical composition. Therefore, the rate at which welds cool and transform from austenite following solidification exerts a strong influence on their properties. In turn, cooling rate is dependent upon the conditions of welding. (Refs. 12, 17–20, 28–30).

The results presented in Section 3 showed, as expected, the variation of heat input produced changes in the all-weld-metal microstructure and mechanical properties.

In spite of the variations obtained in the mechanical properties, all the test specimens produced from the E10018-M electrode satisfied the AWS requirements, regardless of the value of heat input used, at least within the range employed in this work (1.3 to 2.1 KJ/mm) — Fig. 5. Therefore, with this electrode, it is possible to weld with a current varying from 140 to 185 A without the risk of not satisfying the requirements, according to Fig. 6. Thus, the versatility of this electrode is excellent.

With the E12018-M electrode, the situation is somewhat different. Figure 5 shows that the tolerance to heat input variations is smaller than the range employed in this work: no higher than 0.3 KJ/mm. The maximum heat input variation for E11018-M electrode, from Ref. 1, was 0.4 KJ/mm. This means that the admissible current variation for the electrode to satisfy the AWS requirements, would be approximately 15 A; see Fig. 6 (for E11018-M, 20 A was found—Ref. 1). This is a very demanding condition when one considers the variations usually found in the equipment calibration. The manufacturer would find it necessary to specify the exact parameters to be used with each different batch of electrodes, due to the expected unavoidable alloy variation that is obtained with the same formula. These changes in weld metal composition depend on the characteristics of the production facilities, how stringent the raw material specifications are, the quality system employed, etc. It can be seen that the current tolerance leading to tensile results within the AWS standard is large enough for the E10018-M. On the other

hand, the situation for the E11018/12018-M is completely different. Required tensile properties are only obtained within a very narrow heat input range.

Figure 6 points to still another fact: the ratio between the yield strength and tensile strength (YS/TS) increased from E10018-M to E12018-M. Typically, for

- E10018-M it is 0.87;
- E11018-M it is 0.93;
- E12018-M it is 0.96.

So, as the tensile strength rises, there is a smaller range in which to vary the heat input.

It was found in Ref. 2, that as Mn increased, the difference between yield strength and tensile strength decreased. On the other hand, in Ref. 3, where the tensile properties were increased by adding C instead of Mn, that difference was approximately constant or slightly lower. From Ref. 4, it can be seen that the addition of Cr did not alter the difference between YS and TS for all the Cr values considered. When Mn increased from nominal 1.0% to 1.5%, this difference was reduced, but it remained constant again for all the Cr levels for the same Mn content. The main difference between the chemical composition of deposits made from E10018-M and E12018-M electrodes is the addition of Cr, but there is also a small increase in Mn and Ni. This suggests that the overall increase of alloy content — not CR — is the cause for the convergence of yield and tensile strengths in the case under study.

Table 8 shows the percentage of variation of yield strength with respect to the mean value of the yield strength range required by AWS standard for the three electrodes. It can be observed that as the yield strength increases, the percentage of variation decreases, thus rendering the

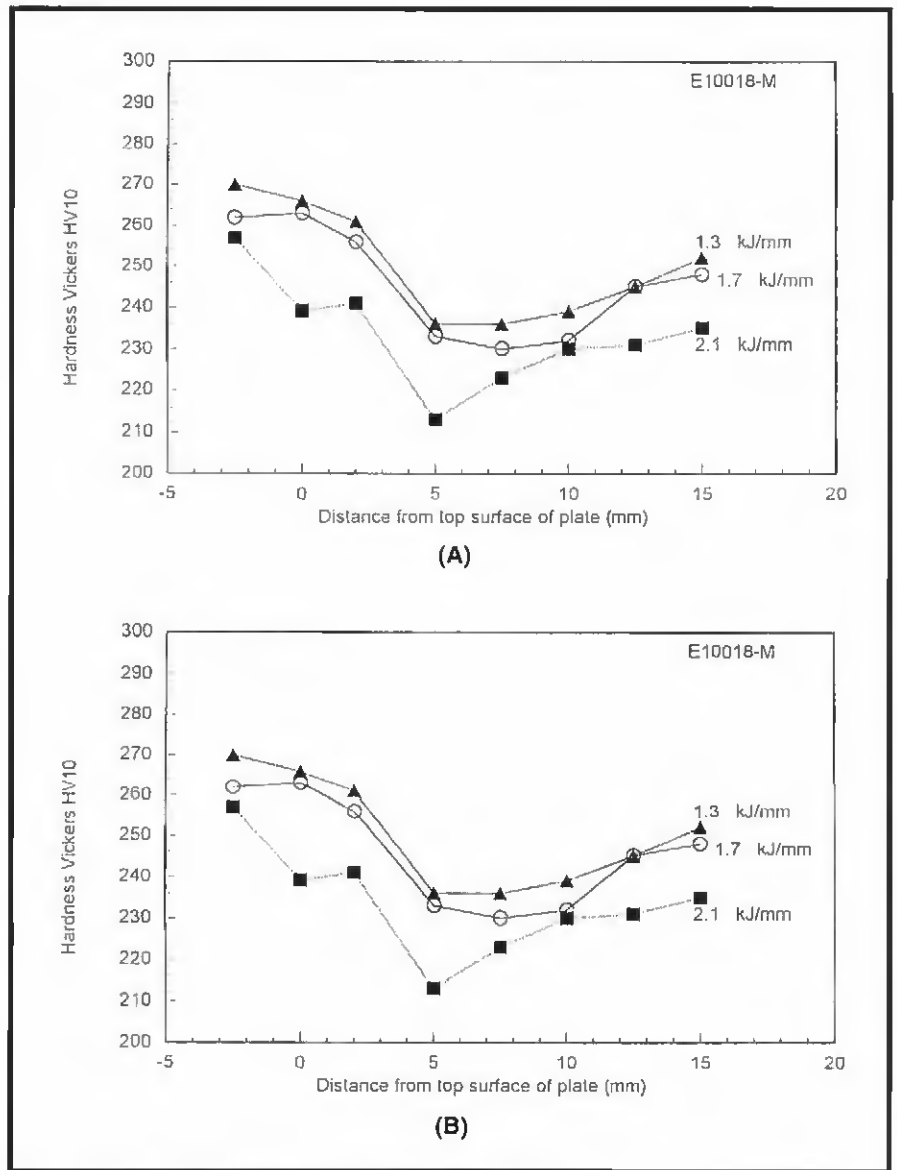


Fig. 4 — All-weld-metal hardness values: A — E10018-M; B — E12018-M.

Table 7 — All-Weld-Metal Mechanical Properties

	Heat Input kJ/mm	Condition	Tensile Strength (N/mm <sup>2</sup> )	Yield Strength (N/mm <sup>2</sup> )	Elongation (%)	Charpy V-Notch at -51°C (J)	
						Obtained Values	AWS Average
E10018-M	2.1	Hot	724	632	23.4	54-57-50-54-56	55
	1.7	Medium	760	660	22.8	57-58-55-56-54	56
	1.3	Cold	766	665	22.0	62-86-72-77-69	73
AWS requirements			690 min	610-690	20 min		27 min
E11018-M (Ref. 1)	2.2	Hot	736-732	669-669	22.8-23.4	49-54-60-54-58	55
	2.0	Medium	764-764	724-705	24.2-23.0	65-58-57-72-48	60
	1.6	Cold	811-809	774-766	20.3-22.8	31-51-53-36-47	45
AWS requirements			760 min	680-760	20 min		27 min
E12018-M	2.1	Hot	796	754	20.7	57-44-65-53-56	55
	1.6	Medium	845	814	19.7	35-62-50-39-66	50
	1.2	Cold	895	866	19.0	50-55-56-50-62	54
AWS requirements			830 min	745-830	18 min		27 min



## Hardness

- With the increase of heat input, the hardness values decreased; the E12018-M electrode had the highest hardness, as expected.

We thus conclude that the AWS all-weld-metal test assemblies with E12018-M electrodes must be performed under strict control and with very precise heat input to obtain reproducible results that satisfy the AWS requirements. These facts must be considered when the procedure test coupons and production weldments are performed.

## AWS A5.5-81 and ANSI/AWS A5.5-96

- This study was performed according to AWS A5.5-81 requirements. Chemical composition and mechanical properties requirements of the two versions of A5.5 standard are the same, but the designs of the Groove Weld Test Assembly for Mechanical Properties and Soundness of Weld Metal are slightly different. This difference may account for variations in tensile properties results. In the opinion of the authors, the all-weld metal behavior general tendency will be the same if the new design is used to evaluate the variation of tensile properties with heat input, but this cannot be assured without the performance of adequate tests.

## Acknowledgments

The authors wish to thank Conarco Alambres y Soldaduras SA for their permission to carry out this work, Eng. J. Sosa, Metallurgist of R&D, Conarco SA, for the metallographic study, Ms. Daniela Mayoral for editing this paper and Ms. María del Carmen Petrucelli for her permanent assistance in the performance of this work. Special thanks is given to Eng. Luis de Vedia for his invaluable help.

## References

1. Vercesi, J., and Surian, E. 1996. The effect of welding parameters on high-strength SMAW all-weld-metal — Part 1: AWS E11018-M. IIW/IIS Doc II-A-915-94. *Welding Journal* 75(6): 191-s to 196-s.
2. Surian, E., Trotti, J., Cassanelli, A. N., and de Vedia, L. A. 1987. Influence of Mn content on mechanical properties and microstructure of a high strength SMA electrode weld metal. IIW/IIS Doc. II-A-724-87.
3. Surian, E., Trotti, J., Herrera, R., and de Vedia, L. A. 1991. Influence of C on mechanical properties and microstructure of weld metal from a high strength SMA electrode. *Welding Journal* 70(6): 133-s to 140-s.

**Table 8 — Percentages of Variation of Yield Strength with Respect to the Medium Value of the Yield Strength Range Required by AWS Standard for the Three Electrodes**

Electrode	AWS Yield Strength Required Range (N/mm <sup>2</sup> )	Yield Strength Required Range Medium Value (N/mm <sup>2</sup> )	Yield Strength Range (N/mm <sup>2</sup> )	% Yield Strength (from Medium Value)
E10018-M	610–690	650	80	±6.2
E11018-M	680–760	720	80	±5.6
E12018-M	745–830	787.5	85	±5.4

4. Surian, E., Trotti, J., Cassanelli, A. N., and de Vedia, L. A. 1992. Influence of chromium on mechanical properties and microstructure of weld metal from a high strength SMA electrode. IIW/IIS Doc. II-1204-92. *Welding Journal* 73(3): 45-s to 53-s.

5. AWS A5.5-81. *Specification for Low-Alloy Steel Covered Arc Welding Electrodes*. American Welding Society, Miami, Fla.

6. ANSI/AWS A5.5-96. *Specification for Low-Alloy Steel Electrodes for Shielded Metal Arc Welding*. American Welding Society, Miami, Fla.

7. Abson, D. J., Duncan, A., and Pargeter, R. J. Guide to the light microscopy examination of ferrite steel weld metals. IIW/IIS Doc. IX-1533-88.

8. Van Nassau, L., and van der Mee, V. Nitrogen in manual metal arc welding. WRC Bulletin, N 369, Dec. 1991/Jan. 1992.

9. Boniszewski, T. *Self-Shielded Arc Welding*. Abington Publishing, Cambridge, England, p. 31.

10. Evans, G. M. 1979. The effect of heat input on the microstructure and properties of C-Mn all-weld-metal deposits. IIW/IIS Doc. II-A-490-79. 1982. *Welding Journal* 61(4): 125-s to 132-s.

11. Evans, G. M. 1979. Effect of electrode diameter on the microstructure and properties of C-Mn all-weld-metal deposits. IIW/IIS Doc. II-A-469-79. 1982. *Welding Review* 1(2), 4–8.

12. Gianetto, J. A., Smith, N. J., McGrath, J. T., and Bowker, J. T. 1992. Effect of composition and energy input on structure and properties of high strength weld metals. *Welding Journal* 71(11): 407-s to 419-s.

13. Evans, G. M. 1988. The influence of molybdenum on the microstructure and properties of C-Mn all-weld-metal deposits. *Join. Mat.* 1(5): 239-s to 246-s.

14. Evans, G. M. 1989. The effect of chromium on the microstructure and properties of C-Mn all-weld-metal deposits. *Weld. Met. Fab.* 57(7): 346–358.

15. Jorge, J. C. J., Souza, L. F. G., Rebello, J. M. A., and Evans, G. M. 1994. Effect of chromium on the microstructure/toughness relationship in C-Mn-Mo weld deposits. IIW/IIS Doc. II-A-930-94.

16. Bott, I. de S. Souza, L., Jorge, J. C., and Surian, E. 1994. Microstructural evaluation of a high strength steel weld metal with varying Cr content by means of scanning electron microscopy. IIW/IIS Doc. II-A-936-94.

17. Smith, N. J., McGrath, J. T., Gianetto, J. A., and Orr, R. F. 1989. Microstructure/

mechanical property relationships of submerged arc welds in HSLA 80 steel. *Welding Journal* 68(3): 112-s to 120-s.

18. Oldland, P. T., Ramsay, C. W., Matlock, D. K., and Olson, D. L. 1989. Significant features of high strength steel weld metal microstructures. *Welding Journal* 68(4): 158-s to 168-s.

19. Stout, R. D., McLaughlin, P. F., and Strunck, S. S. 1969. Heat treatment effects on multi-pass welds. *Welding Journal* 48(4): 155-s to 160-s.

20. Lyttle, J. E., Dorschu, K. E., and Fragetta, W. A. 1969. Some metallurgical characteristics of tough high strength welds. *Welding Journal* 48(11): 493-s to 498-s.

21. *Welding Consumables*. Catalogue, Kobe Steel, Kobelco.

22. Filler materials for manual and automatic welding. *ESAB Welding Handbook*, 4th ed.

23. Liu, S., and Olson, D. L. 1986. The role of inclusions in controlling HSLA steel weld microstructure. *Welding Journal* 65(6): 139-s to 149-s.

24. Ferrant, M., and Farrar, R. A. 1982. The role of oxygen rich inclusions in determining the microstructure of weld metal deposits. *Journal of Materials Science*, 17: 3293–3298.

25. Grong, O., and Matlock, D. K. 1996. Microstructural development in mild and low-alloy steel weld metals. *Int. Metals Review* 31(1): 27–48.

26. Surian, E. S., and Boniszewski, T. 1992. Effect of oxygen content on Charpy V-notch toughness in 3% Ni steel SMA weld metal. *Welding Journal* 71(7): 263-s to 268-s.

27. Abson, D. J., and Pargeter, R. J. 1987. Factors influencing the as-deposited strength, microstructure and toughness of manual arc welds suitable for C-Mn steel fabrication. IIW Doc. II-1092-87.

28. Strunck, S. S., and Stout, R. D. 1972. Heat treatment effects in multipass weldments of a high strength steel. *Welding Journal* 51(10): 508-s to 520-s.

29. Glover, A. G., McGrath, J. T., Tinkler, M. J., and Weatherly, G. C. 1977. The influence of cooling rate and composition on weld metal microstructures in a C/Mn and a HSLA steel. *Welding Journal* 56(9): 267-s to 273-s.

30. Dorschu, K. E. 1968. Control of cooling rates in steel weld metal. *Welding Journal* 47(2): 49-s to 62-s.